Available online at www.sciencedirect.com
SCIENCE DIRECT®
Geomorphology 73 (2006) 16–32
GEOMORPHOLOGY
www.elsevier.com/locate/geomorph

Quaternary landscape evolution in the San Jacinto fault zone, Peninsular Ranges of Southern California: Transient response to strike-slip fault initiation

Rebecca J. Dorsey *, Joshua J. Roering

Department of Geological Sciences 1272 University of Oregon, Eugene, OR 97403, United States

Received 25 October 2004; received in revised form 20 June 2005; accepted 20 June 2005
Available online 3 November 2005

Abstract

Well-constrained case studies of transient landscape response to external forcing are needed to improve our understanding of erosion processes in tectonically active mountain belts. The Peninsular Ranges portion of the San Jacinto fault zone (SJFZ) is an excellent location for such a study because it displays pronounced geomorphic disequilibrium resulting from initiation of a major strike-slip fault in the past 1.0 to 2.5 million years. We recognize two geomorphic domains in this region: (1) a relict low-relief upland domain consisting of broad flat valleys and low-gradient streams and (2) very steep, rough topography with deeply incised canyons and retreating erosional knickpoints. Pleistocene sediments exposed along and near the SJFZ include fluvial conglomerate, sandstone, and mudstone, with weak paleosols and west- to NW-directed paleocurrents. These sediments accumulated in a low-gradient stream system (represented by domain 1) during an early phase of slip in the SJFZ, prior to the modern phase of erosion and degradation (domain 2). Late Pliocene or early Pleistocene initiation of the SJFZ triggered a wave of headward erosion and stream capture that is still migrating NW along the fault zone. Using the total distance that capture points have migrated along the fault zone and a range of possible ages for fault initiation, the rate of knickpoint retreat is estimated at ~12 to 44 km/my.

To explore the signal of transient geomorphic response to fault initiation, we analyzed 23 tributaries along an ~20-km portion of the main fault valley within domain 2. The analysis reveals three zones with distinctive morphologies: (1) strongly convex longitudinal profiles in the NW, (2) a large (ca. 5–6 km^2) landslide in the central zone, and (3) concave tributaries in the SE with profile complexity decreasing and catchment area increasing from NW to SE. The distribution of these zones suggests close spatial and temporal association of active fault slip, bedrock incision, deep-seated landslides, and erosional modification. The fundamental driving force behind these processes is profound geomorphic disequilibrium resulting from initiation of the SJFZ. We suggest that landslides may have played a significant role in shaping the morphology of this fault zone, and that the influence of landslides may be underestimated in areas where characteristic landforms and deposits are obscured by later erosion and faulting.

Keywords: Geomorphology; Strike-slip fault; San Jacinto; Transient response; Stream capture; Landslides

1. Introduction

Recent studies of tectonic geomorphology have focused on efforts to constrain rates, processes, and controlling parameters of bedrock erosion in tectonically active mountain belts (see review in Whipple, 2004).

* Corresponding author. Fax: +1 541 346 4692.
E-mail addresses: rdorsey@uoregon.edu (R.J. Dorsey), jroering@uoregon.edu (J.J. Roering).

0169-555X/$ - see front matter © 2005 Elsevier B.V. All rights reserved.
doi:10.1016/j.geomorph.2005.06.013

Our present understanding of landscape response to external forcing in these settings is derived largely from modeling studies, which indicate that the rate of erosion resulting from a discrete change in boundary conditions is controlled by a complex set of factors including annual rainfall, bedrock lithology, fracture pattern, magnitude of base-level drop, rate of rock uplift, and relative importance of fluvial and hillslope processes (e.g., Howard et al., 1994; Sklar and Dietrich, 1998, 2004; Whipple and Tucker, 1999; Whipple et al., 2000; Simpson and Schlunegger, 2003; Densmore et al., 2003). In spite of these advances, rates of erosion and knickpoint retreat are difficult to predict from theory because of poorly understood nonlinear relationships between model parameters (e.g., Whipple and Tucker, 1999; Crosby and Whipple, in press). Surficial features that form at intermediate timescales (10^4–10^6 years) often dominate tectonically active landscapes, yet field-based studies of fluvial response to external forcing at this timescale are rare (e.g., Blum and Tornqvist, 2000; Schlunegger, 2002; Matmon et al., 2003; Bowman et al., 2004; Pearce et al., 2004). Thus, our ability to test emerging models for geomorphic evolution in active mountain belts is presently limited.

Landsliding is known to exert a strong influence on bedrock erosion and sediment discharge in seismically active settings (Keefer, 1994; Hovius et al., 1997, 1998, 2000; Hervé and Ritz, 1999; Strecker and Marrett, 1999). In a dynamic feedback between fluvial and hillslope processes, channel incision into bedrock results in slope oversteepening and failure, and material delivered by landslides is transported through river channels to areas of deposition (e.g., Allen and Hovius, 1998; Allen and Densmore, 2000; Hovius et al., 2000). Armoring of channels by landslide-derived blocks and boulder lags may inhibit channel incision and enhance the role of large floods (e.g., Baker and Kale, 1998; Hewitt, 1998; Korup, 2004), although the relative importance of small versus large events is poorly known. In addition to modulating long-term erosion in steady-state mountain belts, landslides can accomplish rapid growth of river catchments in young, pre-steady state settings (Hovius et al., 1998), and they may dominate the landscape response to changes in fault kinematics in

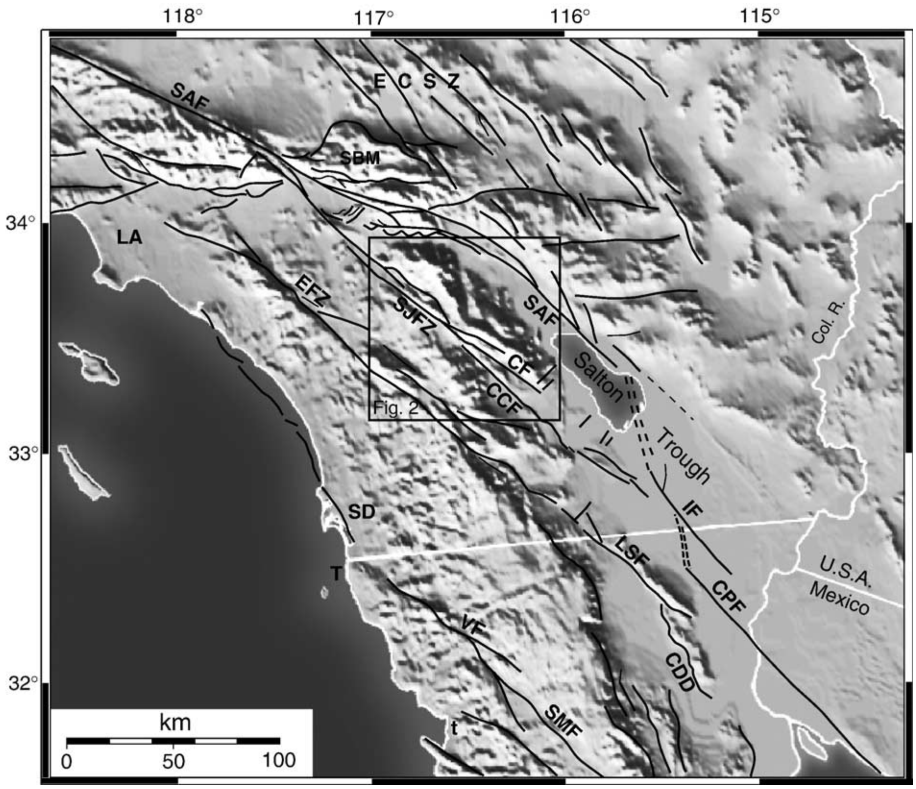

Fig. 1. Shaded relief map of southern California and northwestern Mexico showing mountain ranges and active faults. Box shows location of Fig. 2. CCF, Coyote Creek fault; CF, Clark fault; CDD, Cañada David detachment fault; CPF, Cerro Prieto fault; E, Ensenada; ECSZ, eastern California shear zone; EFZ, Elsinore fault zone; IF, Imperial fault; LA, Los Angeles basin; LSF, Laguna Salada fault; SAF, San Andreas fault; SBM, San Bernardino Mountains; SD, San Diego; SJFZ, San Jacinto fault zone; SMF, San Miguel fault; VF, Vallecitos fault.

active thrust belts (e.g., Strecker and Marrett, 1999). In active strike-slip settings, significant relief can be generated over short timescales such that landslides may be a primary factor in the evolution of associated orogens. The topographic legacy of large mass movements in these areas is largely unconstrained, confounding our ability to assess their role in topographic development.

This paper describes a study of Pleistocene landscape evolution in the Peninsular Ranges portion of the San Jacinto fault zone (SJFZ), southern California (Figs. 1 and 2). The SJFZ provides an excellent laboratory for studying the transient geomorphic response to tectonic forcing because the fault zone is young and seismically active, has good access and age control, and contains a rich record of Quaternary sedimentation and erosion. This study integrates data from sedimentology, stratigraphy, and process geomorphology, with additional information from prior work on structure, petrology, and tectonics in the fault zone. We have identified a relict uplands landscape occupied by gentle slopes and low-energy fluvial deposits that is presently being attacked by channel incision and headward erosion along the fault zone. Reconstruction of the pre-faulting landscape is accomplished through correlation of bedrock markers and topographic features, allowing us to infer the influence of fault-zone initiation on changes in the regional stream system through time. Channel morphology along the fault zone is analyzed through qualitative examination of DEMs and quantitative analysis of longitudinal profiles and slope–area relations for tributaries along the main fault valley. We propose a hypothesis for geomorphic evolution in the fault zone that highlights the effects of pronounced disequilibrium related to late Pliocene or early Pleistocene initiation of the San Jacinto fault.

2. Study area

The San Jacinto fault zone is a complex system of strike-slip fault segments connected by releasing and

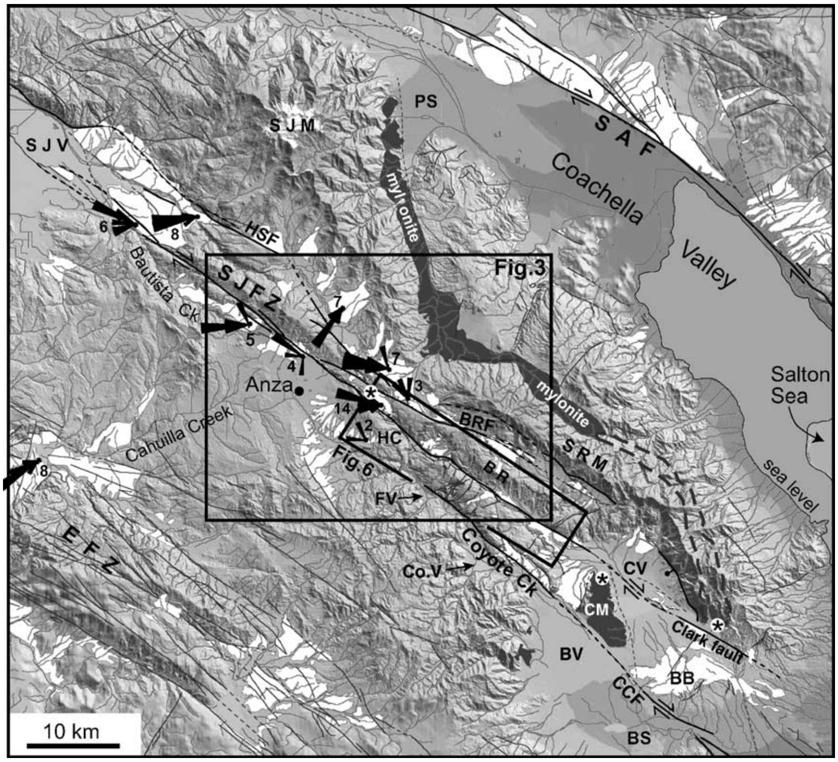

Fig. 2. Shaded-relief DEM showing topography, faults, and Pleistocene sediments in the Peninsular Ranges portion of the San Jacinto fault zone (SJFZ). White patches are Pleistocene sediments, known as Bautista Beds in the mountainous parts of the fault zone. All other areas are crystalline bedrock, including mylonite (labeled), or alluviated valleys and lowlands. Rose diagrams show paleocurrent data collected from Pleistocene sediments (Fig. 5); numbers indicate number of measurements at each site. Asterisks mark correlation points used to estimate distance and rate of knickpoint migration along the fault zone (see Discussion). BB, Borrego Badlands; BC, Bautista Creek; BR, Buck Ridge; BRF, Buck Ridge fault; BS, Borrego Sink; BV, Borrego Valley; CCF, Coyote Creek fault; CM, Coyote Mountain; CV, Clark Valley; Co.V, Collins Valley; EFZ, Elsinore fault zone; FV, Figtree Valley; HC, Horse Canyon; HSF, Hot Springs fault; PS, Palm Springs; SAF, San Andreas fault; SJFZ, San Jacinto fault zone; SJM, San Jacinto Mountain; SJV, San Jacinto Valley; SRM, Santa Rosa Mountains.

restraining bends and stepovers that extends from San Bernadino in the NW to the Salton Trough and Imperial Valley in the SE (Figs. 1 and 2; Sharp, 1967; Sanders, 1989; Sanders and Magistrale, 1997). The geometric complexity of the fault zone is characteristic of young, disorganized strike-slip faults with limited total displacement (Wesnousky, 1986, 1988). Previous studies of the SJFZ in the Peninsular Ranges have focused on geologic mapping and bedrock petrology (Sharp, 1967; Hill, 1984), fault-kinematic analysis (Sharp, 1975; Sanders and Magistrale, 1997), Quaternary slip rates using offset stratigraphic and geomorphic markers (Sharp, 1981; Rockwell et al., 1990), and faulting controls on Quaternary geomorphology and sedimentation (Morton and Matti, 1993; Kendrick et al., 2002; Dorsey, 2001, 2002; Ryter, 2002). Relatively little is known about regional-scale physiography and drainage networks in the Peninsular Ranges and their relationship to initiation and growth of the SJFZ.

Although the SJFZ is known to be geologically young, its age is poorly constrained between about 1.0 and 2.5 Ma. The older age is possible based on estimates of Holocene and late Pleistocene slip rates (10–13 mm/year; e.g., Sharp, 1981; Prentice et al., 1986; Rockwell et al., 1990) and total strike-slip offset (21–26 km; Sharp, 1967; Hill, 1984; Dorsey, 2002). A younger age (1.0 to 1.5 Ma) has been inferred from geologic mapping and stratigraphic studies (Morton and Matti, 1993; Matti and Morton, 1993; Dorsey, 2001) and morphometric analysis that suggested that the Pleistocene slip rate may be faster than 20 mm/year (Kendrick et al., 2002). Geophysical and isotopic mapping shows that the fault zone formed along preexisting faults and crustal weaknesses in the Peninsular Ranges batholith when structural complications in San Gorgonio Pass transferred slip away from the San Andreas fault (Langenheim et al., 2004).

3. Descriptive physiography

The SJFZ in the Peninsular Ranges is characterized by steep fault-controlled ridges and deep canyons juxtaposed against large areas of relatively high elevation and low relief (Figs. 2 and 3). The town of Anza sits at 1200 m elevation in a broad valley that separates NW-flowing Bautista Creek from SE-flowing Coyote Creek. Cahuilla Creek is a low-gradient stream that flows WSW through Anza Valley into drainages of the Elsinore fault zone. Coyote Creek occupies a deep canyon that follows a complex route through the fault zone. From the northwestern Santa Rosa Mountains, the main channel of Coyote Creek flows NW along the NE side of Buck Ridge fault to Horse Canyon, where it passes through a large bend, cuts across an active fault block, and flows SE along the Clark fault (Fig. 3). Southeast of Horse Canyon, the main fault valley is obstructed by high topography related to a restraining bend in the Clark fault and the toe of a large landslide (Sharp, 1967). This obstruction appears to have deflected Coyote Creek south to the Coyote Creek fault, which the modern channel follows SE to Borrego Valley at the western margin of the Salton Trough (Fig. 2). Borrego valley is an actively subsiding alluvial basin at 140 m elevation, ~1000 m below Anza (Bartholomew, 1970; Ryter, 2002).

Two geomorphic domains are recognized in and near the fault zone: (i) high-elevation, low-relief areas with broad valleys and low-gradient streams, including Cahuilla Creek and its tributaries (Figs. 3 and 4A); and (ii) very steep, rough topography with deeply incised canyons of Bautista Creek, Coyote Creek, and their tributaries (Figs. 3 and 4B,C). Domain 1 is interpreted as a "relict landscape" that formed under stable conditions prior to the onset of active erosion recorded in the "modern landscape" of domain 2 (e.g., Schoenbohm et al., 2004). Terwilliger valley is a beheaded valley in domain 1 that has been isolated by modern erosion from its original sediment source in the high Santa Rosa Mountains (Fig. 4A). Low-lying outcrops of Cretaceous tonalite and granodiorite exposed in road cuts west of Anza (domain 1) reveal a deep saprolitic weathering zone mantled by up to 5 m of loose granitic grus at the base of the Pleistocene Bautista beds. This regolith is part of a regionally extensive Cenozoic weathering surface that is recognized over a large area in southern California (e.g., Allen, 1957; Spotila and Sieh, 2000). In contrast, bedrock exposures in deep canyons of domain 2 are fresh and unweathered, reflecting active erosion in those areas (Fig. 4B,C). The boundary between the two domains is marked by the upstream ends of deep canyons where erosional knickpoints and escarpments reflect ongoing headward erosion and stream capture (Fig. 3). Erosion in this boundary zone has created fresh cliff exposures of Pleistocene fluvial deposits in Horse Canyon and along the western margin of Vandeventer Flat (Fig. 4).

In summary, the DEM and field observations show that the high-elevation, relict landscape of domain 1 is presently being attacked by headward erosion in domain 2. The boundary between the two domains is marked by a zone of active knickpoints that are migrating NW along the SJFZ into the high Peninsular Ranges. As discussed below, we infer that modern headward erosion and ongoing stream capture reflect

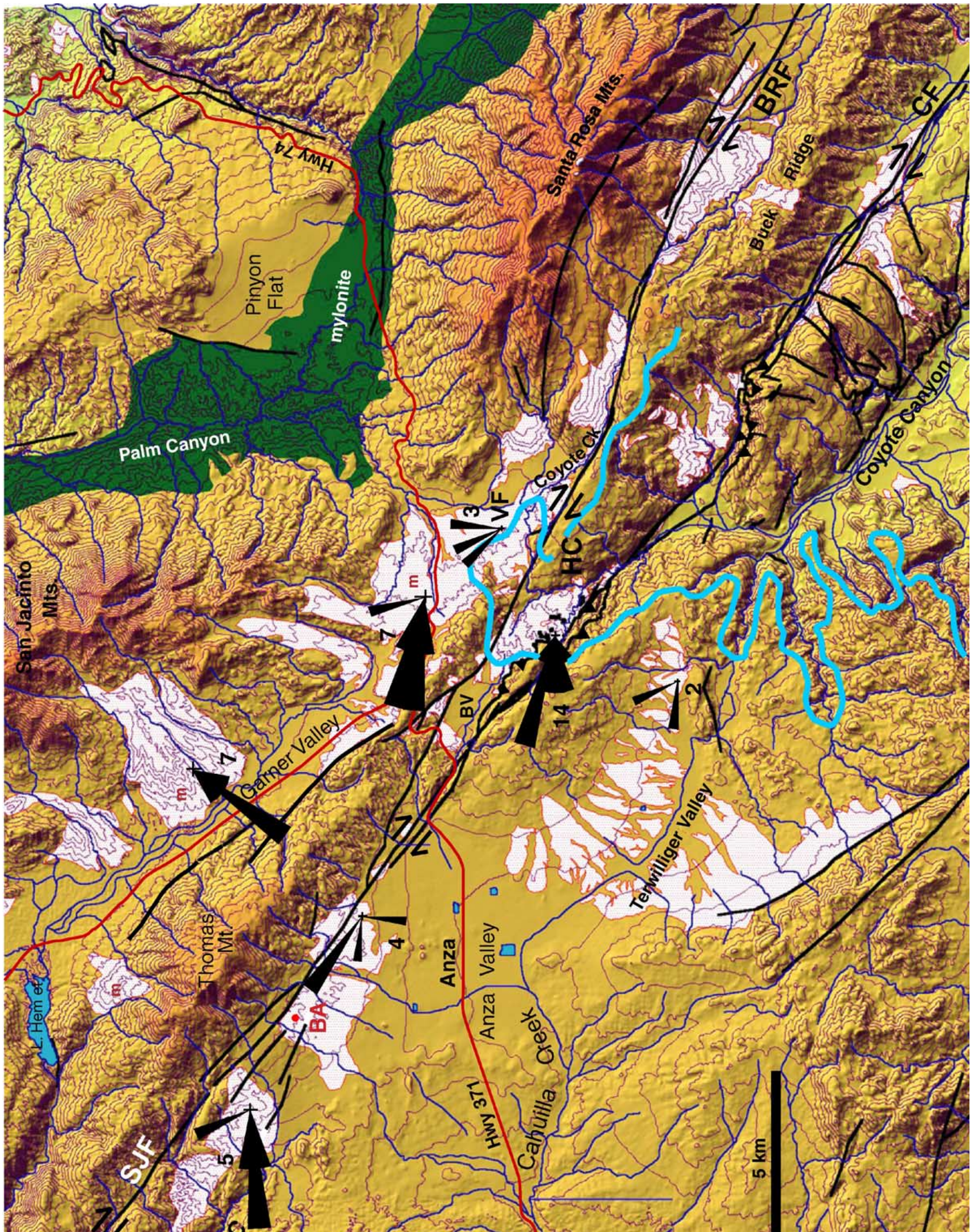
Santa Rosa Mts.
BRF
CF
Buck Ridge
Pinyon Flat
mylonite
Hwy 74
Palm Canyon
Coyote Ck
Coyote Canyon
VF
HC
San Jacinto Mts.
Garner Valley
BV
Terwilliger Valley
Thomas Mt
Anza
Anza Valley
Anza Creek
Cahuilla Creek
Hwy 371
BA
SJF
BC
5 km

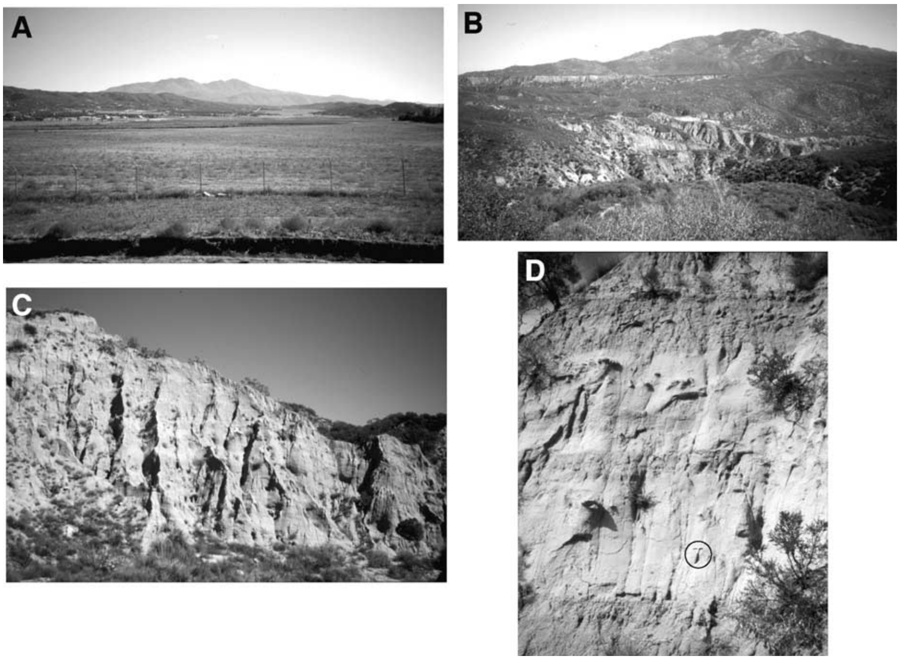

Fig. 4. Photos of the Anza-Horse Canyon area. (A) View looking approximately east from upper Terwilliger valley, near paleocurrent rose, across beheaded upper end of valley toward original source in the Santa Rosa Mountains (see Fig. 3). (B) View looking ENE at deeply incised Pleistocene sediments in upper Horse Canyon (foreground), Santa Rosa Mountains (skyline on right), and erosional escarpment at the west edge of Vandeventer Flat (thin light strip in left-center; Fig. 3). (C) Fine-grained Pleistocene sediments (arkosic sandstone and conglomeratic sandstone) exposed in badlands topography of Horse Canyon. (D) Fine-grained fluvial sediments exposed in erosional escarpment at edge of Vandeventer Flat (Fig. 3), showing sharp-based channel sandstones with cross bedding, fining-upward grain size trends, and weakly developed paleosols. Hammer (circled) is 32.5 cm long.

a geomorphic disequilibrium that was triggered by late Pliocene or early Pleistocene initiation of the San Jacinto fault zone.

4. Pleistocene stratigraphy

Pleistocene sediments exposed in and near the mountainous portions of the SJFZ belong to a wide-spread sequence of sandstone, mudstone, and conglomerate known as Bautista Beds (Figs. 2 Figs. 3 Fig. 4C,D; Frick, 1921; Sharp, 1967). In the lower Coyote Creek area, Bautista Beds include landslide breccia, conglomerate, sandstone, mudstone, and an upper thick unit of weakly consolidated gravel (Sharp, 1967; Dorsey, 2002). In the Peninsular Ranges, Bautista Beds strata are sub-horizontal to gently dipping, with notable exceptions where they are moderately to strongly deformed by faults and folds of the fault zone. The stratigraphic thickness is highly variable, thinning to zero against topographic highs and thickening to ~300 to 400 m in low areas and paleovalleys. The 760-ka Bishop ash has been mapped in sandstone and mudstone facies of Bautista Beds at two localities: (i) north of Anza where the ash is interbedded with claystone and sandstone near the San Jacinto fault (Sharp, 1967, 1981); and (ii) in the Coyote Badlands where it is interbedded in the lower part of a thick faulted section of sandstone and conglomerate (Sharp, 1967; Dorsey, 2002). Samples of ash from both localities were analyzed for trace-element geochemistry and identified as the Bishop ash by Sarna-Wojcicki et al. (1980). This places a useful

Fig. 3. Color DEM with shaded relief showing topography, faults, and Pleistocene sediments (white patches) in the Anza-Horse Canyon area and Santa Rosa mylonite (green belt) east of there. Areas not labeled with white or green are underlain by Cretaceous plutonic rocks and pre-Cretaceous metamorphic rocks (on hillslopes) or Quaternary to modern alluvium (in valleys). Rose diagrams show paleocurrent data (this study; Fig. 5). Bold blue line shows approximate location of boundary between the two domains, marked by migrating knickpoints, knickzones, and erosional escarpments. Contour interval is 50 m. This image illustrates the contrast between high-elevation, low-relief areas of domain 1 (relict landscape; Anza and Terwilliger valleys), and deep canyons and gullies of domain 2 (modern active landscape; Horse Canyon and Coyote Canyon). BA, Bishop Ash locality; BC, Bautista Creek; BRF, Buck Ridge fault; BV, Burnt Valley; CF, Clark fault; HC, Horse Canyon; m, mylonite clast localities; SJF, San Jacinto fault (NW of where CF and BRF merge); VF, Vandeventer Flat. Location shown in Fig. 2.

constraint on the age of Bautista Beds, which Sharp (1967) recognized as a coherent package of laterally correlable and once-contiguous stratigraphy.

Deposits of the Bautista Beds in the Peninsular Ranges are laterally variable and include sandy conglomerate, arkosic pebbly sandstone, sandstone, siltstone, mudstone, and claystone (Sharp, 1967, 1981; this study). Trough cross-bedding, channel structures, planar stratification, and clast imbrications are common in sandstone and conglomerate facies. In some localities, deposits are organized into 1- to 5-m-thick fining-up intervals of cross-bedded channelized sandstone with a pebbly lag above an erosional base, grading up through silty fine-grained sandstone into mudstone with weakly developed paleosols (Fig. 4D). Paleosols are recognized by the presence of reddish mudstones with weak ped structures and calcareous rhizocretions. Other sites contain interbedded pebble conglomerate, pebbly sandstone, and sandstone with planar bedding, low-angle cross bedding, and broad lenticular channel geometries. These features record deposition in a network of low-gradient fluvial channels and adjacent floodplains. Deposits at the base of the steep western slopes of the San Jacinto Mountains contain poorly sorted, unstratified, matrix-rich pebble, cobble, to small-boulder conglomerate with minor sandstone interbeds and no cross-bedding, indicative of debris flow deposition in alluvial fans. Several sites (labeled “m” in Fig. 3) contain abundant distinctive clasts of mylonite that were derived from the Santa Rosa mylonite, now exposed on the steep east flank of the San Jacinto Mountains. Paleocurrent data show overall transport toward the west, away from the Santa Rosa and San Jacinto Mountains, with a moderate amount of directional scatter (Fig. 5).

In many locations (e.g., Horse Canyon; north of Anza; and south of Lake Hemet; Fig. 3), Pleistocene fluvial lithofacies and paleocurrents are unrelated to nearby active faults and steep fault-related topography. At Horse Canyon, sand-dominated fluvial deposits with minor gravel show transport toward the WNW, opposite the direction of stream flow in modern gullies incised into the Pleistocene sediments. North of Anza, Bishop Ash-age sediments consist of fine-grained sandstone, siltstone, and claystone (fluvial to fluvio-lacustrine facies) that are deformed by tight to overturned folds adjacent to the San Jacinto fault (Sharp, 1981). These tightly folded sediments are overlain along an angular unconformity by two fluvial gravel units, the younger of which contains clasts that were used by Sharp (1981) to estimate amount and rate of offset on the San Jacinto fault. Overlying the gravel units at this locality is a mantling unit of coarse bouldery colluvium and landslide deposits related to modern steep topography on the SW flank of Thomas Mt. (Fig. 3). In the small patch of Bautista Beds located due south of Lake Hemet (Fig. 3), cross-bedded fine-grained sandstone, siltstone, and mudstone (low-energy fluvial facies) are perched on the steep northern flank of Thomas Mt., well above the area of modern fluvial processes. These fine-grained fluvial sediments are overlain by a thick mantle of bouldery colluvium and landslide debris similar to that seen north of Anza. In these examples, the low-gradient fluvial conditions recorded in Bishop Ash-age sediments have been replaced by modern steep slopes and incised gullies resulting from active fault-related uplift and erosion.

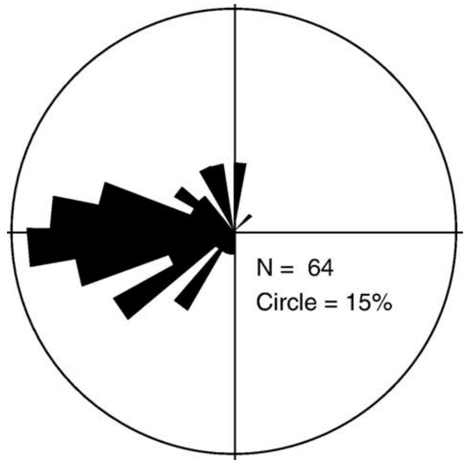

Fig. 5. Rose diagram of all paleocurrent data collected for this study, from cross bedding and channel axes in sandstone, and clast imbrications in conglomerate. Data for individual locations are shown in Figs. 2 and 3.

The above observations indicate that post-depositional deformation in the San Jacinto fault zone has significantly deformed, eroded, and changed the spatial distribution of Bishop Ash-age sediments. On Thomas Mt., these sediments have been mostly stripped off by erosion related to active faulting and uplift. Fine-grained fluvial deposits perched on the steep flanks of this active uplift indicate that a low-energy river system once covered the area now occupied by Thomas Mt. Despite these large post-depositional changes, the paleocurrent data reveal some similarity between fluvial transport directions and fault trend (Figs. 2, 3 and 5). This suggests that stream flow was partially deflected by strike-slip faults and that these faults, or earlier strands, were active during deposition of Bautista Beds sediments.

5. Tributary channel morphology

5.1. Methods

We analyzed a series of tributary channels along a portion of the SJFZ to document the transient geomorphic response to fault initiation and related stream capture. The area selected for this analysis is located within domain 2 and covers a distance of about 20 km along the Clark fault, where large variations are seen in the shape and width of the main fault valley, geometry of the fault, and morphology of adjacent hillslopes (Fig. 6). Because the NW end of this area is located near the zone of active stream capture and erosional escarpments and these features are migrating NW up the fault zone through time, along-fault changes in morphology should contain information about the evolution of erosional processes in the fault zone. Surface morphology is revealed in a shaded-relief DEM, channel profiles for tributaries on the NE side of the fault valley, and slope–area plots for the same tributaries (Figs. 6–8). The upper end of each profile is defined as the highest point where channel morphology is recognized from plan-view crenulation (tight curvature) of elevation contours seen on 1:24,000 scale topographic maps. The lower end of each profile was picked where the stream channel exits the incised valley and enters either the main stem of the through-going trunk stream or a flat valley bottom.

The morphology of river channel profiles is a reflection of fluvial erosion and deposition in response to different types of external forcing. Channel gradient has been shown to decrease systematically with increasing drainage area, reflecting the concave nature of most river longitudinal profiles (e.g., Gilbert, 1877; Mackin, 1948). An empirical power–law relationship has been proposed, such that slope varies with area according to $S = k_s A^{-\theta}$, where S is channel gradient, k_s is a steepness index, and θ is the channel concavity index (Howard and Kerby, 1983; Sklar and Dietrich, 1998; Whipple and Tucker, 1999). Although theories that explain the slope–area relationship remain elusive, k_s is commonly inferred to reflect climate, tectonic, and lithologic factors (e.g., Whipple, 2004). All else being equal, k_s should vary in concert with rate of uplift or base-level lowering (Dietrich et al., 2003), and several topography-based studies have supported this notion (Merritts and Vincent, 1989; Stock and Montgomery, 1999; Snyder et al., 2002b; Kirby and Whipple, 2001; Kobor and Roering, 2004). These studies have shown that k_s values vary by over 8–9 orders of magnitude, reflecting significant differences in uplift rate, bedrock lithology, and other factors. In contrast, values of θ typically do not vary significantly (Kirby et al., 2003; Snyder et al., 2002a), suggesting that landscapes with highly variable θ values have experienced a complex history of forcing by lithologic properties and/or tectonic, climatic, or erosional processes. Here, we use the simple power–law slope–area relationship to quantify the topographic manifestation of coupled tectonic and surface processes in the SJFZ.

5.2. Geologic features and geomorphic data

The area of this analysis includes a large landslide and an ~4-km-long restraining bend in the Clark fault (Fig. 6). The restraining bend consists of several west- to NW-striking thrust faults that dip 15° to 79° to the south and SW, contain abundant fault gouge and crushed rocks, and juxtapose crystalline bedrock directly against Quaternary sediment (Sharp, 1967). Map relations, including prominent outliers (klippen) of crystalline rock resting on Quaternary sediments, provide evidence that the thrust faults post-date the landslide and accommodated significant horizontal translation (~0.5 to 1.0 km) of the hanging wall toward

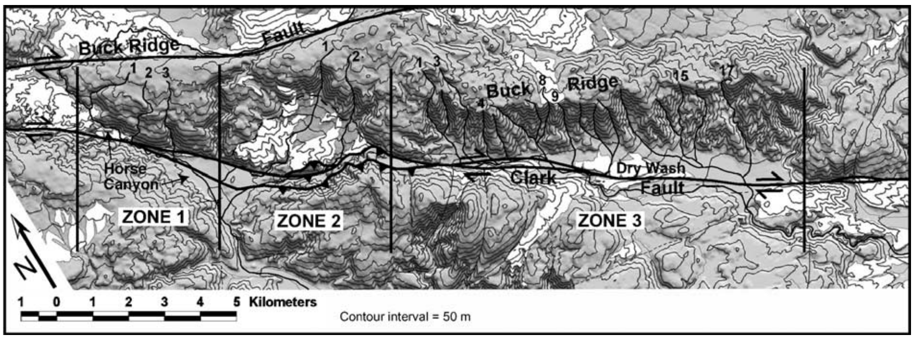

Fig. 6. Shaded-relief DEM of part of the San Jacinto fault zone, showing geomorphic zones 1–3 and tributaries on NE side of the fault valley that were analyzed in this study (Figs. 7–9). Location of map shown in Fig. 2. See text for discussion.

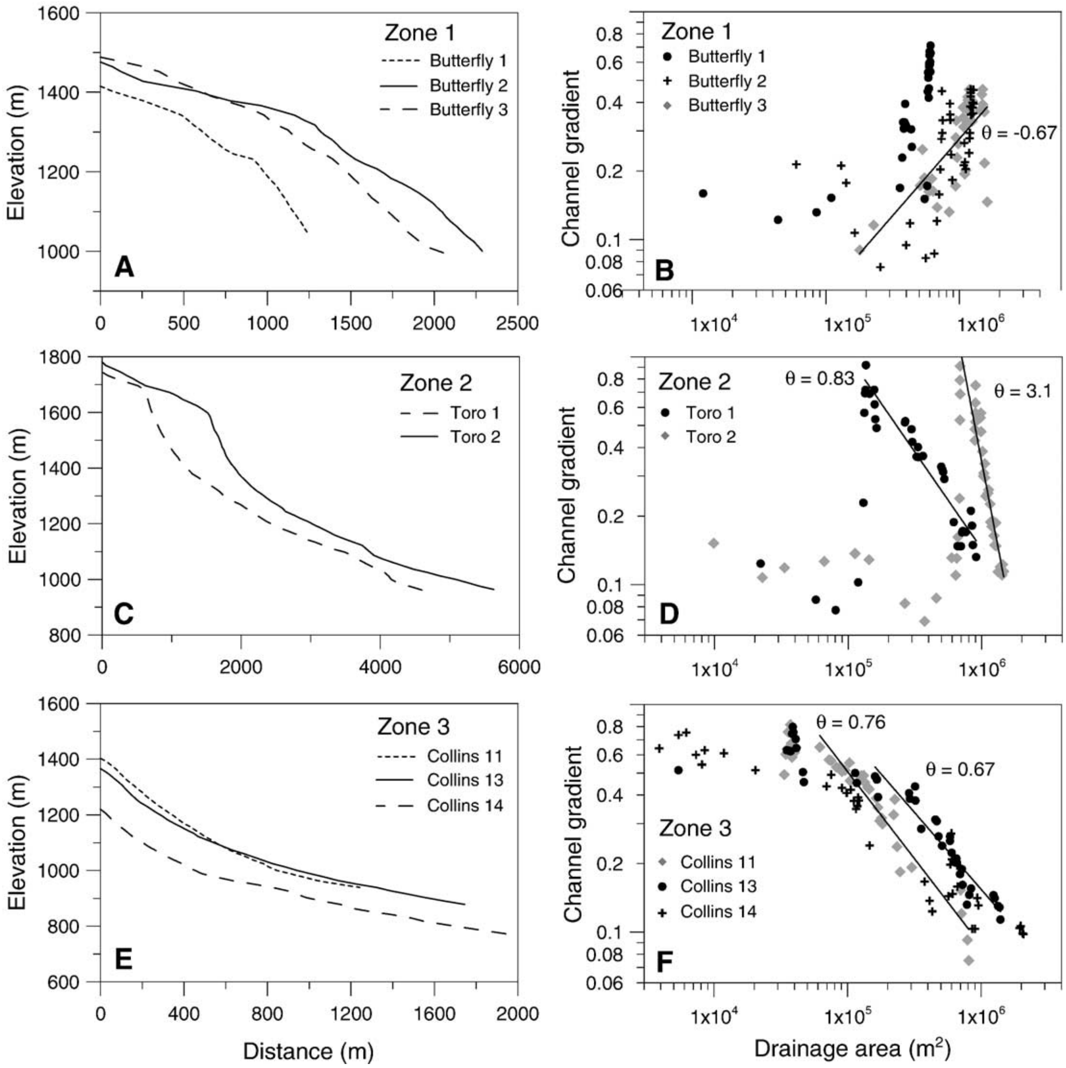

Fig. 7. Tributary channel profiles and slope–area plots for zones 1 and 2 and representative profiles from zone 3. Note contrast in channel profiles for the three zones: convex in zone 1; characteristic landslide geometry in zone 2; concave in zone 3 with less concavity than zone 2.

the NE (Sharp, 1967). These features, combined with high topography SW of the thrust faults and a local drainage divide near the apex of the restraining bend, suggest that a continuous valley once followed the Clark fault through this area and was later closed by NE-directed thrusting of crystalline rocks across the valley floor. Alternatively, the drainage divide SE of the landslide may be an original feature and there has never been a trunk stream that followed the Clark fault in this area. Based on the observed map and structural relations, we favor the first interpretation of a once-continuous fault valley that was more recently disrupted by NE-directed thrusting in the restraining bend.

The features summarized above define three geomorphic zones, all within the active landscape of domain 2, on the NE side of the fault valley: (1) steep convex-up slopes in the NW that are being undercut and oversteepened by erosion in Horse Canyon; (2) a large (5–6 km^2) landslide with characteristic head scarp, run-out path, and hummocky topography in the toe; and (3) ~10-km-long zone in which the Clark fault valley widens to the SE, and steep concave-up tributary streams flow from a linear ridge (Buck Ridge) directly into Dry Wash valley (Fig. 6).

Tributary channel profiles in zone 1 are characterized by distinctive convex-up geometry (Fig. 7A) and slope–area curves that reveal an overall positive correlation between channel gradient and catchment area (negative θ; Fig. 7B). In zone 2, two streams that flow across the landslide reveal characteristic head-

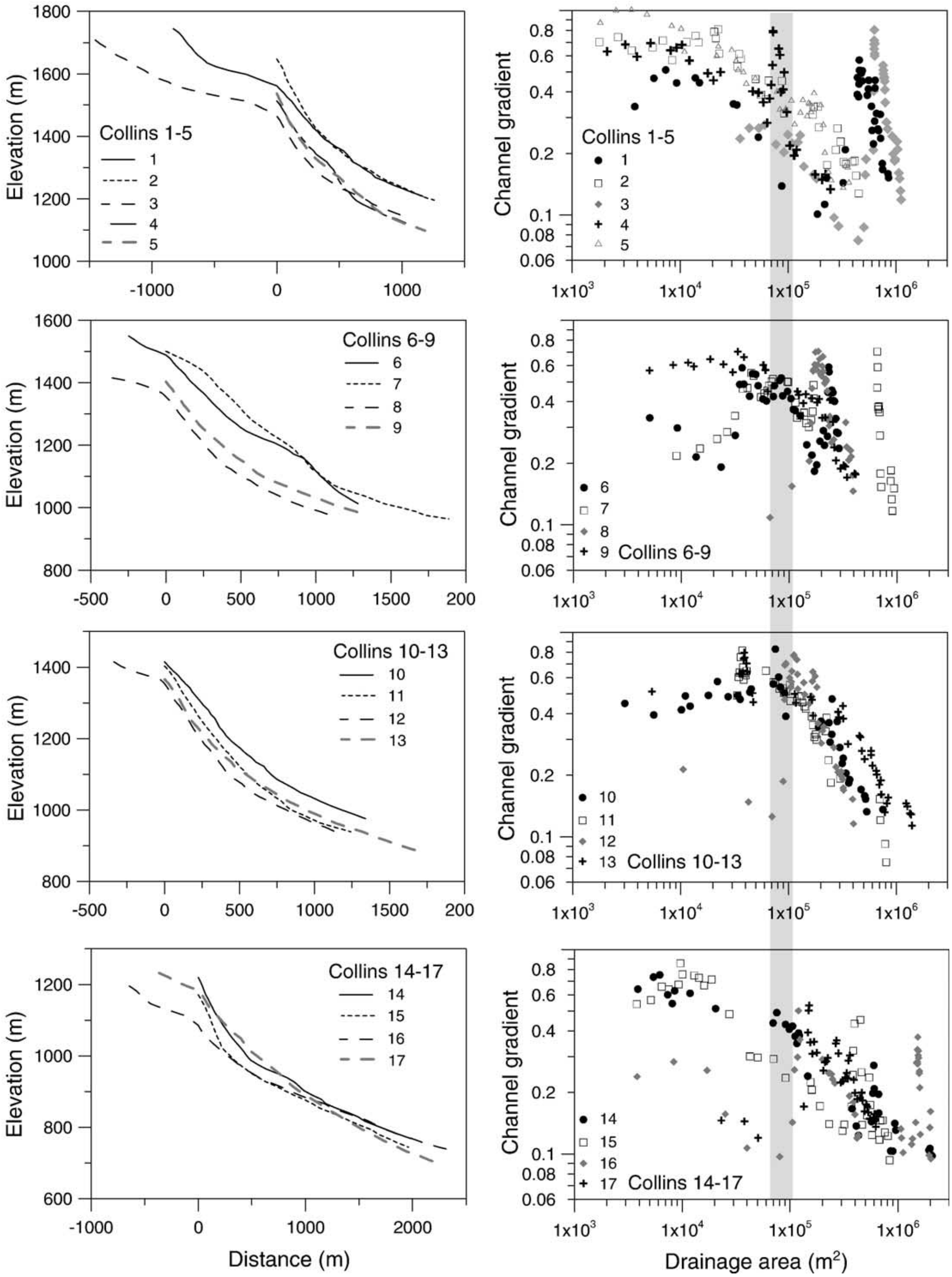

Fig. 8. Tributary channel profiles and slope–area plots for all tributaries in zone 3. Shaded vertical bar in right-hand plots indicates approximate lower limit of sporadic low slopes seen in upper flat portions of some tributaries (shown in left column of plots).

scarp, run-out, and toe geometries produced by landslide translation and deformation (Fig. 7C). Slope–area plots in zone 2 show localized steep negative trends (large positive values of θ) that reflect high concavity of the headscarp and run-out portions of the landslide (Fig. 7D). Representative tributary profiles in zone 3 are concave, with reduced concavity relative to zone 2; most profiles do not show the distinctive morphological

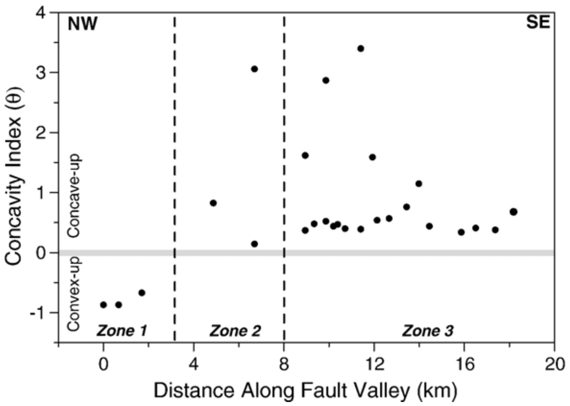

Fig. 9. Plot of tributary channel concavity index (θ) as a function of distance along the main fault valley. Theta values reflect convex channel profiles (negative θ) in zone 1, landslide morphology (headscarp and slide deposit) in zone 2, and southeastward change to more uniform morphology in zone 3 where θ converges toward ~0.4 to 0.6.

signature of landsliding seen in zone 2 (Fig. 7E,F). Plots of all tributaries in zone 3 (Fig. 8) show a slight decrease in maximum gradient and reduction in geometric complexity from NW to SE along the fault valley and show a systematic increase in the length of tributary channels below an upper flat segment (where present). These changes parallel a southeastward increase in the width of the SW flank of Buck Ridge and widening of the Dry Wash fault valley (Fig. 6).

Concavity index (θ) was calculated for all tributaries and plotted as a function of distance along the main fault valley (Fig. 9). Negative θ values in zone 1 reflect the strongly convex-up channel longitudinal profiles in that area. The shift to positive and variable θ in zone 2 results from extreme concavity in the headscarp of the landslide and nearly linear channel profile in the slide deposit. θ in zone 3 shows an overall NW-to-SE decrease in range and maximum values, converging to ~0.4 to 0.6 in the SE (Fig. 9). This reflects decreasing concavity and increasing uniformity of tributary morphology toward the southeast.

6. Discussion

6.1. Fault zone reconstruction

Data presented above indicate that Pleistocene sediments of the Anza–Horse Canyon area accumulated in a low-gradient stream network that flowed west and NW from the San Jacinto and Santa Rosa Mountains toward the Pacific coast during an early phase of slip in the SJFZ. Areally restricted deposits of poorly sorted, matrix-rich conglomerate were deposited by gravelly debris flows in alluvial fans sourced in the high San Jacinto Mountains. Deep canyons and gullies are currently migrating NW up the fault zone and cutting into Pleistocene fluvial deposits in a complex network of retreating knickpoints, gullies, and erosional escarpments. Modern erosion in this setting reflects pronounced disequilibrium produced when a low-gradient stream system that once flowed along a long gentle path was captured by new streams flowing down a much shorter, steeper, and energetically favored path to sea level. In this example, new streams began to attack the older relict landscape when strike-slip offset in the fault zone disrupted a preexisting regional drainage divide and created a new fault valley. This style of base-level drop does not require a drop in sea level or uplift of the relict uplands landscape, though one or both of those factors could also be involved.

Fig. 10A is a schematic reconstruction of streams that flowed across the Peninsular Ranges (relict landscape of domain 1) during Pliocene time, prior to initiation of the SJFZ. The reconstruction is constrained by remnants of the pre-SJFZ drainage divide in the modern Santa Rosa, Coyote, and San Ysidro Mountains, and by correlation of mylonite across the Clark and Coyote Creek faults (Fig. 2; Sharp, 1967). The general consistency of bedrock and topographic correlations suggests that, prior to offset in the SJFZ, a regional drainage divide separated low-gradient west-flowing streams in the west from steep short drainages that flowed east to the Salton Trough (Fig. 10A). The pre-SJFZ divide apparently was maintained by slow uplift and broad westward tilting in the footwall of a regional detachment fault system that was active from late Miocene to early Pleistocene time (Axen and Fletcher, 1998). Regional topography probably resembled that of northern Baja California (NW Mexico) where the Sierra San Pedro Martir Mts. are being uplifted and gently tilted to the west in the footwall of a large active normal fault at the east margin of the range (Brown, 1978; Gastil et al., 1975).

Fig. 10B shows the inferred configuration of the region during deposition of Pleistocene fluvial sediments (Bautista Beds), after initiation of the SJFZ but prior to onset of erosion in the Horse Canyon area. Although the timing of fault initiation is not well known, the consequences of this event are clearly seen in the stratigraphic and geomorphic record. Early fault slip produced broad sags and depressions that resulted in accumulation of fluvial sediment and partial deflection of streams toward the NW. Strike-slip fault offset breached the former regional drainage divide, creating a new stream that flowed SE along the fault

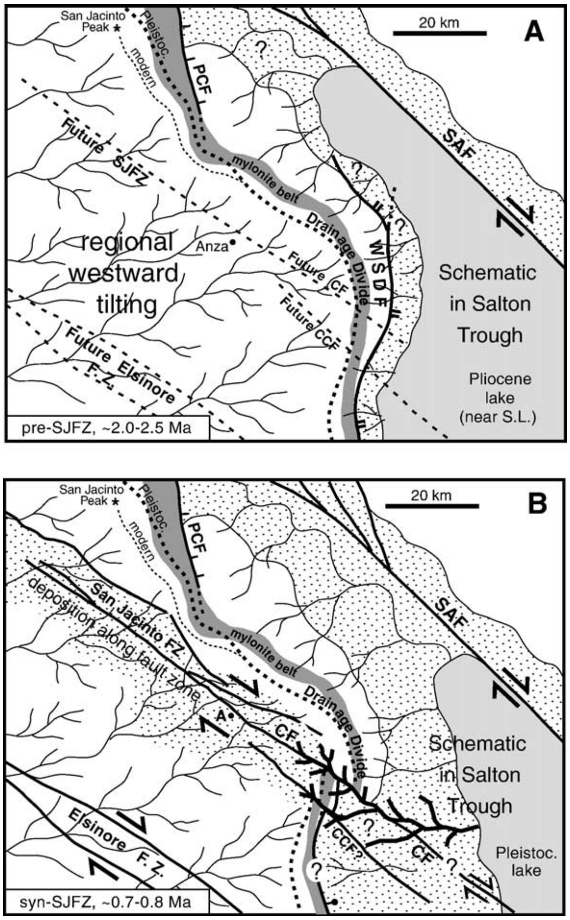

Fig. 10. Schematic diagram showing proposed reconstruction of the San Jacinto fault zone. (A) Regional westward tilting and west-flowing streams in footwall of west Salton detachment fault (WSDF) during Pliocene time, prior to initiation of SJFZ, as represented by relict landscape of domain 1. (B) Pleistocene deposition in Peninsular Ranges, sometime after initiation of the fault zone and prior to arrival of migrating headward erosion in the Anza-Horse Canyon area.

valley to the Salton Trough. Because of the short distance to sea level, the new stream network was much steeper than the west-flowing river system and therefore was energetically favored. This initiated a wave of headward erosion and aggressive stream capture that propagated NW along the fault zone (Fig. 10B), similar to tectonically forced drainage reversal and divide migration documented in the Costa Rican volcanic arc (Gardner et al., 1992; Marshall et al., 2003). Sometime after 760 ka, the migrating drainage divide arrived in the Horse Canyon area, and resultant stream capture initiated deep erosion of Pleistocene sediments and underlying bedrock. This process is active today at the edges of the Terwilliger and Anza valleys, where remnants of the west-flowing stream system (Cahuilla Creek) are in the process of being captured by Coyote Creek and its tributaries (Figs. 2 and 3). The time lag between initiation of the SJFZ and onset of erosion in the Anza–Horse Canyon area reflects the time required for knickpoints to migrate along the fault zone from their point of initiation at the former drainage divide.

6.2. Rate of knickpoint migration

The rate of erosional knickpoint and escarpment retreat in the SJFZ can be estimated from the distance of migration and the time elapsed since initiation of the fault zone, assuming that initiation of the fault zone is the event that triggered knickpoint migration. We also assume that the local drainage divide at the zone 2–3 boundary (Fig. 6) reflects recent structural disruption of a formerly continuous valley along the Clark fault (see Section 5.2). The total distance of knickpoint migration is ~30 km as measured along the Clark fault from the pre-SJFZ drainage divide at Borrego Mt. to the area of active stream capture points at the south edge of Burnt Valley (asterisks in Fig. 2). This distance appears to be a minimum because rocks on the NE side of the Clark fault are moving SE toward Borrego Mt. (on the SW side of the fault). An alternate measurement, from the pre-SJFZ divide on the NE side of the Clark fault to the area of modern stream captures at the edge of Burnt Valley (Fig. 2), gives an along-fault distance of ~44 km. These values are considered to bracket the total distance of knickpoint migration. The age of the SJFZ is uncertain, with estimates ranging between about 2.5 and 1.0 Ma (see summary in Introduction). Using this range of ages and distances, the long-term average rate of erosional knickpoint migration along the fault zone is estimated to be ~12–44 km/my.

The rate of knickpoint migration estimated above is significantly faster than that calculated for retreating erosional escarpments at passive continental margins (~0.05 to 2.0 km/my; Seidl et al., 1996; Weissel and Seidl, 1997, 1998; Matmon et al., 2002). It is slower than two known late Pleistocene examples: (1) in SE Spain where headward erosion migrated 20 km in 100 ky (equivalent to a long-term rate of 200 km/my; Mather et al., 2002), and (2) headward erosion of fault-controlled canyons in the active Costa Rican arc >80 km in 320–400 ky (~200 to 250 km/my) (Marshall et al., 2003). Comparison of knickpoint migration rates at different timescales is difficult, however, and should be viewed with caution. As noted by Matmon et al. (2002), escarpment retreat rates at rifted continental margins are initially very rapid and slow considerably as the margins stabilize. Thus, long-term averages used to calculate erosional retreat rates at old passive margins may substantially underestimate rates that are active during early stages of escarpment retreat. The relatively rapid migration rate documented here appears to reflect the initial pulse of rapid erosion that is expected for young active settings.

Mylonite clasts in gravel at several localities ("m" in Fig. 3) provide a unique constraint on escarpment retreat because they are presently isolated from bedrock mylonite by the modern drainage divide and there are no significant areas of mylonite on the west flank of the San Jacinto Mountains (Fig. 3; Hill, 1984). This appears to require an ~5 km westward shift in the position of the drainage divide since deposition of the gravel (~760 ka), suggesting erosional retreat of the eastern San Jacinto escarpment at a rate of ~6.5 km/my. This is slower than the rate of knickpoint migration calculated for the fault zone (12–44 km/my), as can be expected for erosion of unfaulted bedrock. If the eastward dip on the mylonite is only slightly steeper than the eastern slope of the San Jacinto Mountains, a shorter distance and slower rate of erosional retreat would be sufficient to isolate the mylonite-bearing gravel from its original bedrock source.

6.3. Evolution of regional topography

The history of uplift in the Peninsular Ranges is poorly understood despite abundant interest in this problem. Uplift is not required to trigger erosion in this system, so independent data are needed to constrain the uplift history. Young uplift in the southern Santa Rosa Mountains (e.g., King et al., 2002; Matti et al., 2002) does not require uplift in the rest of the Peninsular Ranges because the Santa Rosa Mountains are separated from areas to the SW by the active Buck Ridge–Santa Rosa fault system (Fig. 2). Published thermochronologic studies of the San Jacinto Mountains have documented crustal cooling and exhumation in late Cretaceous (George and Dokka, 1994) and middle Tertiary (Wolf et al., 1997) times, but did not identify a signal of Plio-Pleistocene cooling. Coarse Pliocene conglomerate in the western Salton Trough requires some topography in the Peninsular Ranges (Dibblee, 1954, 1984; Winker, 1987; Winker and Kidwell, 1996; Axen and Fletcher, 1998), and isotopic data from Pliocene strata suggest the presence of a rain shadow in the Peninsular Ranges by about 2.0 Ma (Cosma et al., 2002).

Raised flights of dated marine terraces in coastal southern California provide evidence for Pleistocene uplift on the western slopes of the Peninsular Ranges at rates of about 0.13–0.35 m/ky (Lajoie et al., 1979; McCrory and Lajoie, 1979; Kennedy et al., 1982; Kern and Rockwell, 1992; Muhs et al., 1992), but the relationship of coastal uplift to the Peninsular Ranges is complicated by active faults and lack of dated terraces inland. Rivero et al. (2000) proposed that uplift of coastal terraces is due to slip on offshore blind thrusts. Others have argued that uplift of the same terraces results from large-scale tectonic processes such as flexural response to rifting that are largely independent of motion on individual faults (Muhs et al., 1992; Orme, 1998; Kier et al., 2001). Geophysical data and modeling show that high topography in the Peninsular Ranges is presently supported by thinning of mantle lithosphere related to extension in the Salton Trough and Gulf of California (Lewis et al., 2000, 2001), but this mechanical model does not provide any constraint on the timing of regional uplift. Thus, the timing and rate of Cenozoic uplift in the Peninsular Ranges, and possible links to coastal deformation, remain poorly known.

6.4. Geomorphic evolution in the fault zone

Stream profiles in Fig. 7 reveal pronounced contrasts in tributary channel morphology along the SJFZ. We infer that convex-up profiles in zone 1 represent steep unstable slopes that existed prior to bedrock failure and emplacement of the landslide in zone 2. This implies very rapid lowering of the fault valley relative to adjacent hillslopes, which prevented the tributaries from establishing concave-up longitudinal profiles. Rapid lowering of elevation along the trunk stream may have resulted from a combination of factors including regional tectonic forcing of local base level (Fig. 10B), strike-slip juxtaposition of pre-existing topographic elements, oblique opening across the fault to form a narrow "rift valley", and/or preferential erosion of crushed and fractured crystalline rock in the fault zone. The close spatial association of features in zones 1 and 2 suggests a time-for-space equivalence in which processes recorded in these two zones represent two stages of geomorphic development that occurred in sequence. We therefore hypothesize that rapid erosion in the fault valley produced steep, unstable convex slopes (Fig. 11A) that were subsequently leveled by the large landslide (Fig. 11B).

We further speculate that the concave channel profiles in zone 3 may have inherited and modified topography created by earlier landslides (Fig. 11C), similar to the process of catchment growth by slope failures and post-landslide erosion documented in Papua New Guinea (Hovius et al., 1998). The large range of concavity index (θ) in zone 2 and the NW part of zone 3 (Fig. 9)

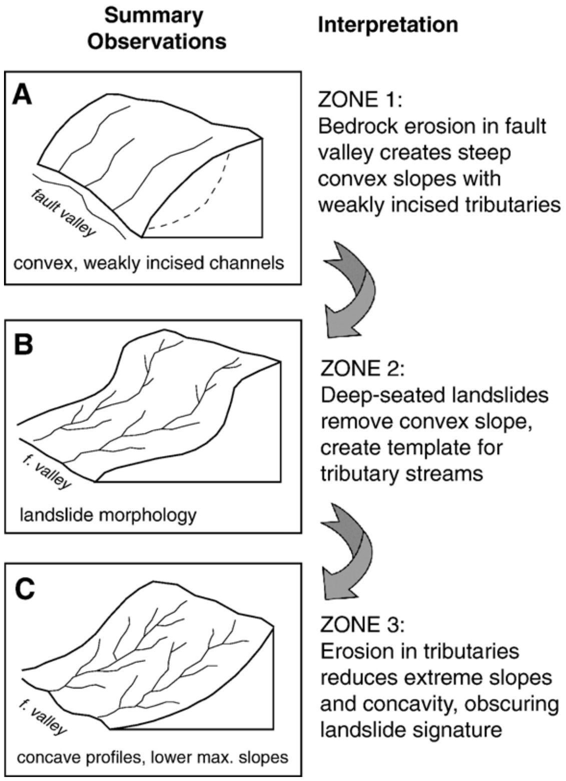

Fig. 11. Speculative time-for-space hypothesis for geomorphic evolution in the San Jacinto fault zone. (A) Convex-up tributary profiles in zone 1 are produced by rapid bedrock incision along the fault. (B) Landslides in zone 2 level unstable slopes and create a topographic template for tributaries. (C) Headward erosion in zone 3 obscures landslide morphology, reducing the extreme slopes and concavity seen in zone 2. These processes are inferred to migrate in succession along the fault zone and are driven by geomorphic disequilibrium related to late Pliocene or early Pleistocene initiation of the fault zone.

reveals variable catchment morphology that suggests a similar origin. In previous studies of established catchments in active orogens, θ values typically cluster between about 0.4 and 0.6 (Whipple, 2004), consistent with our results near the SE margin of the tributary analysis. The southeastward decrease in the range and maximum values of θ in zone 3 appears to reflect lateral expansion of tributaries by headward erosion on the SW flank of Buck Ridge. Thus, we suggest that the three geomorphic zones in Fig. 6 may record a succession of genetically related processes–slope oversteepening, large bedrock landslides, and post-landslide erosional modification–that have migrated NW along the fault zone in the wake of headward-eroding knickpoints. If correct, this would imply that the distinctive morphology and deposits of older landslides have been largely obscured by subsequent erosion and faulting in the active fault zone. Alternatively, the landslide in zone 2 may be a singular event related to local structural and lithologic conditions, and does not necessarily represent a ubiquitous process in this system. However, deep-seated landslides are widely recognized as a common process associated with active faults and steep topography in the eastern Peninsular Ranges (e.g., Sharp, 1967; Pinault, 1984; Morton, 1989; Hart, 1991a,b; Button and Wenk, 1998), and the signs of this process are likely to be transient in a landscape dominated by vigorous erosion on steep hillslopes. The time–space hypothesis for geomorphic evolution in the fault zone is therefore speculative but plausible, and requires further testing.

7. Conclusions

This study documents dynamic links between fault initiation, fluvial incision, knickpoint retreat, and generation of large landslides in the active San Jacinto fault zone. Pleistocene fluvial sediments accumulated in a low-gradient stream system during an early period of slip in the SJFZ, prior to the onset of headward erosion triggered by initiation of the fault in late Pliocene or early Pleistocene time. The lag time between fault initiation and onset of erosion in the Anza–Horse Canyon area reflects the distance that knickpoints migrated along the fault zone from their starting position at the pre-SJFZ drainage divide. The time-averaged rate of knickpoint migration, 12–44 km/my, is intermediate between rates documented in other systems that are older and younger than the SJFZ. This result supports previous inferences that erosion in response to regional base-level perturbation is initially very rapid and slows with time.

Tributary channels along a portion of the fault zone can be grouped into 3 geomorphic zones: (1) strongly convex channel profiles in the NW; (2) a large landslide in the central zone; and (3) concave tributaries in the SE with profile complexity decreasing from NW to SE. Convex channel profiles in zone 1 reflect rapid erosion along the fault valley, and bedrock landslides in zone 2 record leveling of unstable slopes represented in zone 1. First-order streams in zone 3 are modifying a more mature landscape by headward erosion and expansion of tributary catchments. These processes are hypothesized to migrate along the fault through time in response to profound disequilibrium resulting from initiation of the SJFZ. We suggest that landslides may have played a significant role in shaping the morphology of this fault zone. If true, it would imply that the influence of landslides may be underestimated in areas where the characteristic deposits and landforms are quickly obscured by subsequent erosion and faulting.

Acknowledgements

This study benefited from insightful conversations with Kurt Frankel, Susanne Janecke, George Jefferson, Jonathan Matti, Doug Morton, Tom Rockwell, Derek Ryter, and Ray Weldon. Derek Ryter is thanked for assistance in digitizing and processing the DEMs. We thank James Spotila, Jeffrey Marshall, and Richard Marston for thorough and constructive reviews of the manuscript. Support for this research was provided by the National Science Foundation (grants EAR-9805794 and EAR-0125921).

References

Allen, C.R., 1957. San Andreas fault zone in San Gorgonio Pass, southern California. Geological Society of America Bulletin 68, 315–350.

Allen, P.A., Densmore, A.L., 2000. Sediment flux from an uplifting fault block. Basin Research 12, 367–380.

Allen, P.A., Hovius, N., 1998. Sediment supply from landslide-dominated catchments: implications for basin margin fans. Basin Research 10, 19–35.

Axen, G.J., Fletcher, J.M., 1998. Late Miocene–Pleistocene extensional faulting, northern Gulf of California, Mexico and Salton Trough California. International Geology Review 40, 217–244.

Baker, V.R., Kale, V.S., 1998. The role of extreme floods in shaping bedrock channels. In: Tinkler, K.J., Wohl, E.E. (Eds.), Rivers Over Rock, Fluvial Processes in Bedrock Channels, Geophysical Monograph Series, vol. 107. American Geophysical Union, Washington, DC, pp. 153–165.

Bartholomew, M.J., 1970. San Jacinto fault zone in the northern Imperial Valley California. Geological Society of America Bulletin 81, 3161–3166.

Blum, M.D., Tornqvist, T.E., 2000. Fluvial responses to climate and sea-level change; a review and look forward. In: Best, J.L., Fielding, C., Jarvis, I., Mozley, P. (Eds.), Millenium Reviews, Sedimentology, Supplement 47, pp. 2–48.

Bowman, D., Korjenkov, A., Porat, N., Czassny, B., 2004. Morphological response to Quaternary deformation at an intermontane basin piedmont, the northern Tien Shan, Kyrghyzstan. Geomorphology 63, 1–24.

Brown, L.G., 1978. Recent fault scarps along the eastern escarpment of the Sierra San Pedro Martir, Baja California. MS thesis, San Diego State University, San Diego, California, 88 pp.

Button, E.A., Wenk, H.-R., 1998. A geomorphic and engineering evaluation of the eastern Peninsular Ranges between Palm Desert and Martinez Mountain. Abstracts with Programs-Geological Society of America 30 (5), 8.

Cosma, T.N., Smith, A.J., Palmer, D.F., 2002. Uplift of Peninsular Ranges affects terrestrial climate record of enhanced tropical moisture in late Pliocene, Anza-Borrego Desert, California. Abstracts with Programs-Geological Society of America 34 (6), 45.

Crosby, B.T., Whipple, K.X., in press. Knickpoint initiation and distribution in fluvial networks: 236 waterfalls in the Waipaoa River, North Island, NZ. Geomorphology.

Densmore, A.L., Dawers, N.H., Gupta, S., Allen, P.A., Gilpin, R., 2003. Landscape evolution at extensional relay zones. Journal of Geophysical Research-Solid Earth 108 (B5), 2273. doi:10.1029/2001JB001741.

Dibblee Jr., T.W., 1954. Geology of the Imperial Valley region, California, Geology of Southern California. California Division of Mines Bulletin 170, 21–28.

Dibblee, T.W., 1984. Stratigraphy and tectonics of the San Felipe Hills, Borrego Badlands, Superstition Hills, and vicinity. In: Rigsby, C.A. (Ed.), The Imperial Basin: Tectonics, Sedimentation, and Thermal Aspects. Pacific Section SEPM, Los Angeles, CA, pp. 31–44.

Dietrich, W.E., Bellugi, D., Sklar, L.S., Stock, J.D., Heimsath, A.M., Roering, J.J., 2003. Geomorphic transport laws for predicting landscape form and dynamics. In: Iverson, R.M., Wilcock, P. (Eds.), Prediction in Geomorphology. Am. Geoph. Union, Washington, DC, pp. 103–132.

Dorsey, R.J., 2001. Two-stage evolution of the San Jacinto fault zone: crustal response to Pleistocene oblique collision along the San Andreas fault. Eos Trans. AGU Fall Meeting Suppl. 82 (47), 933.

Dorsey, R.J., 2002. Stratigraphic record of Pleistocene initiation and slip on the Coyote Creek fault, lower Coyote Creek, southern California. In: Barth, A. (Ed.), Contributions to Crustal Evolution of the Southwest United States, Geological Society of America Special Paper, vol. 365. Geological Society of America, Boulder, CO, pp. 251–269.

Frick, C., 1921. Extinct vertebrate faunas of the Badlands of Bautista Creek and San Timoteo Canyon, southern California. California University, Department of Geology Bulletin 12, 277–424.

Gardner, T.W., Verdonck, D., Pinter, N.M., Slingerland, R.L., Furlong, K.P., Bullard, T.F., Wells, S.G., 1992. Quaternary uplift astride the Cocos Ridge, Pacific coast Costa Rica. Geological Society of America Bulletin 104, 219–232.

Gastil, R.G., Phillips, R.P., Allison, E.C., 1975. Reconnaissance Geology of the State of Baja California, Geological Society of America Memoir, vol. 140. Geological Society of America, Boulder, CO, 170 pp.

George, P.G., Dokka, R.K., 1994. Major Late Cretaceous cooling events in the eastern Peninsular Ranges, California, and their implications for Cordilleran tectonics. Geological Society of America Bulletin 106, 903–914.

Gilbert, G.K., 1877. Report on the geology of the Henry Mountains (Utah). Publication of the Powell Survey, 160 pp.

Hart, M.W., 1991a. Failure mechanisms of mega-landslides in the Peninsular Ranges of Southern California. Abstracts with Programs-Geological Society of America 23 (5), 126.

Hart, M.W., 1991b. Landslides in the Peninsular Ranges, Southern California. In: Walawender, M.J., Hanan, B.B. (Eds.), Geological Excursions in Southern California and Mexico. San Diego State University, San Diego, California, pp. 349–371.

Hervé, P., Ritz, J.F., 1999. Gigantic paleolandslide associated with active faulting along the Bogd fault (Gobi-Altay Mongolia). Geology 27, 211–214.

Hewitt, K., 1998. Catastrophic landslides and their effects on the Upper Indus streams Karakoram Himalaya, northern Pakistan. Geomorphology 26, 47–80.

Hill, R.I., 1984. Petrology petrogenesis of batholithic rocks, San Jacinto Mountains, Southern California [PhD dissertation]: California Institute of Technology, Pasadena, CA, 731 pp.

Hovius, N., Stark, C.P., Allen, P.A., 1997. Sediment flux from a mountain belt derived by landslide mapping. Geology 25, 231–234.

Hovius, N., Stark, C.P., Tutton, M.A., Abbott, L.D., 1998. Landslide-driven drainage network evolution in a pre-steady-state mountain belt; Finisterre Mountains Papua New Guinea. Geology 26, 1071–1074.

Hovius, N., Stark, C.P., Hao-Tsu, C., Jiun-Chuan, L., 2000. Supply and removal of sediment in a landslide-dominated mountain belt: Central Range Taiwan. Journal of Geology 108, 73–89.

Howard, A.D., Kerby, G., 1983. Channel changes in badlands. Geological Society of America Bulletin 94, 739–752.

Howard, A.D., Dietrich, W.E., Seidl, M.A., 1994. Modeling fluvial erosion on regional to continental scales. Journal of Geophysical Research 99 (B7), 13971–13986.

Keefer, D.K., 1994. The importance of earthquake-induced landslides to long-term slope erosion and slope-failure hazards in seismically active regions. Geomorphology 10, 265–284.

Kendrick, K.J., Morton, D.M., Wells, S.G., Simpson, R.W., 2002. Spatial and temporal deformation along the northern San Jacinto fault, southern California: implications for slip rates. Bulletin of the Seismological Society of America 92, 2782–2802.

Kennedy, G.L., Lajoie, K.R., Wehmiller, J.F., 1982. Aminostratigraphy and faunal correlations of late Quaternary marine terraces Pacific Coast, USA. Nature 299, 545–547.

Kern, J.P., Rockwell, T.K., 1992. Chronology and deformation of Quaternary marine shorelines, San Diego County, California. In: Heath, E., Lewis, L. (Eds.), The Regressive Pleistocene Shoreline in Southern California, South Coast Geological Society Annual Field Trip Guidebook, vol. 20. South Coast Geological Society, Santa Ana, pp. 1–7.

Kier, G.B., Mueller, K., Rockwell, T., 2001. Origin of regional uplift across southern California and northern Baja California. Eos Trans. AGU Fall Meeting Suppl. 82 (47), 1252.

King, T., Cox, B.F., Matti, J.C., Powell II, C.L., Osterman, L.E., Bybell, L.M., 2002. Previously unreported outcrops of Neogene Imperial Formation in southern Santa Rosa Mountains, California, and implications for tectonic uplift. Abstracts with Programs-Geological Society of America 34 (6), 124.

Kirby, E., Whipple, K., 2001. Quantifying differential rock-uplift rates via stream profile analysis. Geology 29, 415–418.

Kirby, E., Whipple, K., Tang, W.Q., Chen, Z.L., 2003. Distribution of active rock uplift along the eastern margin of the Tibetan Plateau: inferences from bedrock channel longitudinal profiles. Journal of Geophysical Research 108 (B4), 2217. doi:10.1029/2001JB000861.

Kobor, J.S., Roering, J.J., 2004. Systematic variation of bedrock channel gradients in the central Oregon Coast Range: implications for rock uplift and shallow landsliding. Geomorphology 62, 239–256.

Korup, O., 2004. Landslide-induced river channel avulsions in mountain catchments of southwest New Zealand. Geomorphology 63, 57–80.

Lajoie, K.R., Kern, J.P., Wehmiller, J.F., Kennedy, G.L., Mathieson, S.A., Sarna-Wojcicki, A.M., Yerkes, R.F., McCrory, P.F., 1979. Quaternary marine shorelines and crustal deformation, San Diego to Santa Barbara, California. In: Abbott, P.L. (Ed.), Geological Excursions in the Southern California Area. San Diego State Univ., San Diego, CA.

Langenheim, V.E., Jachens, R.C., Morton, D.M., Kistler, R.W., Matti, J.C., 2004. Geophysical and isotopic mapping of preexisting crustal structures that influenced the location and development of the San Jacinto fault zone, southern California. Geological Society of America Bulletin 116, 1143–1157.

Lewis, J.L., Day, S.M., Magistrale, H., Eakins, J., Vernon, F., 2000. Regional crustal thickness variations of the Peninsular Ranges Southern California. Geology 28, 303–306.

Lewis, J.L., Day, M.D., Magistrale, H., Castro, R.R., Astiz, L., Robollar, C., Eakins, J., Vernon, F.L., Brune, J.N., 2001. Crustal thickness of the Peninsular Ranges and Gulf Extensional Province in the Californias. Journal of Geophysical Research 106, 13599–13611.

Mackin, J.H., 1948. Concept of the graded river. Geological Society of America Bulletin 5, 463–511.

Marshall, J.S., Idleman, B.D., Gardner, T.W., Fisher, D.M., 2003. Landscape evolution within a retreating volcanic arc Costa Rica, Central America. Geology 31, 419–422.

Mather, A.E., Stokes, M., Griffiths, J.S., 2002. Quaternary landscape evolution: a framework for understanding contemporary erosion SE Spain. Land Degradation & Development 13, 89–109.

Matmon, A., Bierman, P., Yehouda, E., 2002. Pattern and tempo of great escarpment erosion. Geology 30, 1135–1138.

Matmon, A., Wdowinski, S., Hall, J.K., 2003. Morphological and structural relations in the Galilee extensional domain, northern Israel. Tectonophysics 371, 223–241.

Matti, J.C., Morton, D.M., 1993. Paleogeographic evolution of the San Andreas Fault in Southern California: a reconstruction based on a new cross-fault correlation. In: Powell, R.E., Weldon, R.J., Matti, J.C. (Eds.), The San Andreas Fault System: Displacement, Palinspastic Reconstruction, and Geologic Evolution, Geological Society of America Memoir, vol. 178. Geological Society of America, Boulder, CO, pp. 107–159.

Matti, J.C., Cox, B.F., Morton, D.M., Sharp, R.V., King, T., 2002. Fault-bounded Neogene sedimentary deposits in the Santa Rosa Mountains, southern California: crustal stretching or transpressional uplift? Abstracts with Programs-Geological Society of America 34 (6), 124.

McCrory, P.A., Lajoie, K.R., 1979. Marine terrace deformation, San Diego County California. Tectonophysics 52 (1–4), 407–408.

Merritts, D.J., Vincent, K., 1989. Geomorphic response of coastal stream to low, intermediate, and high rates of uplift, Mendocino junction region, northern California. Geological Society of America Bulletin 101, 1373–1388.

Morton, D.M., 1989. Landslides flanking the northeastern Peninsular Ranges and in the San Gorgonio Pass area of southern California. In: Sadler, P.M., Morton, D.M. (Eds.), Landslides in a Semi-Arid Environment with Emphasis on the Inland Valleys of Southern California., Publ. of the Inland Geological Society, vol. 2, pp. 338–355. Redlands, CA.

Morton, D., Matti, M., 1993. Extension and contraction within an evolving divergent strike-slip fault complex: the San Andreas and San Jacinto fault zones at their convergence in Southern California. In: Powell, R.E., Weldon, R.J., Matti, J.C. (Eds.), The San Andreas Fault System: Displacement, Palinspastic Reconstruction, and Geologic Evolution, Geological Society of America Memoir, vol. 178. Geological Society of America, Boulder, CO, pp. 217–230.

Muhs, D.R., Rockwell, T.K., Kennedy, G.L., 1992. Late Quaternary uplift rates of marine terraces on the Pacific coast of North America, southern Oregon to Baja California Sur. Quaternary International 15/16, 121–133.

Orme, A.R., 1998. Late Quaternary tectonism along the Pacific coast of the Californias: a contrast in style. In: Stewart, I.S., Vita-Finzi, C. (Eds.), Coastal Tectonics, Geological Society Special Publication, vol. 146. Geological Society of London, London, pp. 179–197.

Pearce, S.A., Pazzaglia, F.J., Eppes, M.C., 2004. Ephemeral stream response to growing folds. Geological Society of America Bulletin 116, 1223–1239.

Pinault, T.C. 1984. Structure, tectonic geomorphology and neotectonics of the Elsinore fault zone between Banner Canyon and the Coyote Mountains, Southern California. MS thesis, San Diego State University, San Diego, California, 231 pp.

Prentice, C.S., Weldon, R.J., Sieh, K., 1986. Distribution of slip between the San Andreas and San Jacinto faults near San Bernardino, Southern California. Abstracts with Programs-Geological Society of America 18 (2), 172.

Rivero, C., Shaw, J.H., Mueller, K., 2000. Oceanside and Thirtymile Bank blind thrusts: implications for earthquake hazards in coastal southern California. Geology 28, 891–894.

Rockwell, T., Loughman, C., Merifield, P., 1990. Late Quaternary rate of slip along the San Jacinto fault zone near Anza, southern California. Journal of Geophysical Research 95 (B6), 8593–8605.

Ryter, D.W., 2002. Late Pleistocene kinematics of the central San Jacinto fault zone, southern California. PhD dissertation, University of Oregon, Eugene, OR, 137 pp.

Sanders, C.O., 1989. Fault segmentation and earthquake occurrence in the strike-slip San Jacinto fault zone, California. In: Schwartz, D.P., Sibson, R.H. (Eds.), Proceedings of Conference XLV, Workshop on Fault Segmentation and Controls of Rupture Initiation and Termination, U.S. Geological Survey Open-File Report, OF 89-0315, pp. 324–349.

Sanders, C., Magistrale, H., 1997. Segmentation of the northern San Jacinto fault zone Southern California. Journal of Geophysical Research 102, 27453–27467.

Sarna-Wojcicki, A.M., Bowman, H.W., Meyer, C.E., Russell, P.C., Asaro, F., Michael, H., Rowe, J.J., Baedecker, P.A., McCoy, G., 1980. Chemical Analyses, Correlations, and Ages of Late Cenozoic Tephra Units of East-central and Southern California. U.S. Geological Survey Open File Report, OF 80-231, Denver, CO 57 pp.

Schlunegger, F., 2002. Impact of hillslope-derived sediment supply on drainage basin development in small watersheds at the northern border of the central Alps of Switzerland. Geomorphology 46, 285–305.

Schoenbohm, L.M., Whipple, K.X., Burchfiel, B.C., Chen, L., 2004. Geomorphic constraints on surface uplift, exhumation, and plateau growth in the Red River region, Yunnan Province China. Geological Society of America Bulletin 116, 895–909.

Seidl, M.A., Weissel, J.K., Pratson, L.F., 1996. The kinematics of escarpment retreat across the rifted continental margin of SE Australia. Basin Research 12, 301–316.

Sharp, R.V., 1967. San Jacinto fault zone in the Peninsular Ranges of southern California. Geological Society of America Bulletin 78, 705–729.

Sharp, R.V., 1975. En echelon fault patterns of the San Jacinto Fault zone. In: Crowell, J.C. (Ed.), San Andreas Fault in southern California: A Guide to San Andreas Fault from Mexico to Carrizo Plain, Special Report, vol. 118. California Division of Mines and Geology, Sacramento, CA, pp. 147–152.

Sharp, R.V., 1981. Variable rates of late Quaternary strike slip on the San Jacinto fault zone Southern California. Journal of Geophysical Research 86, 1754–1762.

Simpson, G., Schlunegger, F., 2003. Topographic evolution and morphology of surfaces evolving in response to coupled fluvial and hillslope sediment transport. Journal of Geophysical Research 108 (B6), 2300. doi:10.1029/2002JB002162.

Sklar, L., Dietrich, W.E., 1998. River longitudinal profiles and bedrock incision models: stream power and the influence of sediment supply. In: Tinkler, K.J., Wohl, E.E. (Eds.), Rivers Over Rock, Fluvial Processes in Bedrock Channels, Geophysical Monograph Series, vol. 107. American Geophysical Union, Washington, DC, pp. 237–260.

Sklar, L., Dietrich, W.E., 2004. A mechanistic model for river incision into bedrock by saltating bed load. Water Resources Research 40 (6). doi:10.1029/2003WR002496.

Snyder, N.P., Whipple, K.X., Tucker, G.E., Merritts, D.J., 2002a. Interactions between onshore bedrock-channel incision and nearshore wave-base erosion forced by eustasy and tectonics. Basin Research 14, 105–127.

Snyder, N.P., Whipple, K.X., Tucker, G.E., Merritts, D.J., 2002b. Landscape response to tectonic forcing: digital elevation model analysis of stream profiles in the Mendocino triple junction region, northern California. Geological Society of America Bulletin 112, 1250–1263.

Spotila, J.A., Sieh, K., 2000. Architecture of transpressional thrust faulting in the San Bernardino Mountains, southern California, from deformation of a deeply weathered surface. Tectonics 19, 589–615.

Stock, J.D., Montgomery, D.R., 1999. Geologic constraints on bedrock river incision using the stream power law. Journal of Geophysical Research 104 (B3), 4983–4994.

Strecker, M.R., Marrett, R., 1999. Kinematic evolution of fault ramps and its role in development of landslides and lakes in the northwestern Argentine Andes. Geology 27, 307–310.

Weissel, J.K., Seidl, M.A., 1997. Influence of rock strength properties on escarpment retreat across passive continental margins. Geology 25, 631–634.

Weissel, J.K., Seidl, M.A., 1998. Inland propagation of erosional escarpments and river profile evolution across the southeast Australian passive continental margin. In: Tinkler, K.J., Wohl, E.E. (Eds.), Rivers Over Rock, Fluvial Processes in Bedrock Channels, Geophysical Monograph Series, vol. 107. American Geophysical Union, Washington, DC, pp. 189–206.

Wesnousky, S.G., 1986. Earthquakes, Quaternary faults, and seismic hazard in California. Journal of Geophysical Research 91, 12587–12631.

Wesnousky, S.G., 1988. Seismological and structural evolution of strike-slip faults. Nature 335, 340–343.

Whipple, K.X., 2004. Bedrock rivers and the geomorphology of active orogens. Annual Review of Earth and Planetary Sciences 32, 151–185.

Whipple, K.X., Tucker, G.E., 1999. Dynamics of the stream-power river incision model: implications for height limits of mountain ranges, landscape response timescales, and research needs. Journal of Geophysical Research 104, 17661–17674.

Whipple, K.X., Hancock, G.S., Anderson, R.S., 2000. River incision into bedrock: mechanics and relative efficacy of plucking, abrasion, and cavitation. Geological Society of America Bulletin 112, 490–503.

Winker, C.D., 1987. Neogene stratigraphy of the Fish Creek-Vallecito section, southern California: implications for early history of the northern Gulf of California and Colorado delta. PhD dissertation, University of Arizona, Tucson, AZ, 494 pp.

Winker, C.D., Kidwell, S.M., 1996. Stratigraphy of a marine rift basin: Neogene of the western Salton Trough, California. In: Abbott, P.L., Cooper, J.D. (Eds.), Field Conference Guidebook and Volume for the Annual Convention, San Diego, California. Pacific Section, American Association of Petroleum Geologists, Bakersfield, CA, pp. 295–336.

Wolf, R.A., Farley, K.A., Silver, L.T., 1997. Assessment of (U–Th)/He thermochronometry: the low temperature history of Mt San Jacinto, California. Geology 25, 65–68.